Single beam optical tweezers setup with backscattered light detection for three-dimensional measurements on DNA and nanopores

Andy Sischka,[1,a)] Christoph Kleimann,[1] Wiebke Hachmann,[2] Marcus M. Schäfer,[3] Ina Seuffert,[4] Katja Tönsing,[1] and Dario Anselmetti[1]
[1]*Experimental Biophysics and Applied Nanoscience, Faculty of Physics, Bielefeld Institute for Biophysics and NanoScience (BINAS), Bielefeld University, 33615 Bielefeld, Germany*
[2]*Molecular and Surface Physics, Faculty of Physics, Bielefeld Institute for Biophysics and NanoScience (BINAS), Bielefeld University, 33615 Bielefeld, Germany*
[3]*Center for Nanotechnology (CeNTech), Heisenbergstr. 11, 48149 Münster, Germany*
[4]*Fachbereich Physik, University of Konstanz, Fach M621, 78457 Konstanz, Germany*

(Received 25 January 2008; accepted 11 May 2008; published online 18 June 2008)

We introduce a versatile and high precision three-dimensional optical tweezers setup with minimal optical interference to measure small forces and manipulate single molecules in the vicinity of a weak reflective surface. Our tweezers system integrates an inverted optical microscope with a single IR-laser beam that is spatially filtered in an appropriate way to allow force measurements in three dimensions with remarkably high precision when operated in backscattered light detection mode. The setup was tested by overstretching a λ-DNA in *x* and *z* directions (perpendicular and along the optical axis), and by manipulating individual λ-DNA molecules in the vicinity of a nanopore that allowed quantitative single molecule threading experiments with minimal optical interference. [DOI: 10.1063/1.2938401]

I. INTRODUCTION

Measuring small forces in the subpiconewton range with optical tweezers is commonly realized by detecting the forward scattered light of a trapped object (forward scatter mode), which is collected by a condenser lens and projected onto a position sensitive detector, as the condenser objective has to be held at a fixed distance to the trapping objective.[1–9] This requires precise adjustments, and makes it necessary to balance the distance between these two lenses, when moving the trapping objective due to focussing.[10]

Efforts have been made to overcome the condenser lens by using only that light, which is backreflected or backscattered from the trapped object (backscatter mode).[11–14] However, since mostly transparent particles are being trapped, with a refractive index barely higher than their surrounding medium, the available light intensity in reflection mode is considerably less intensive compared to the forward scattered light.[13] Because optical tweezers are commonly operated at wavelengths in the near infrared range,[15] the amount of backscattered light is even less than it would be in visible light spectrum. Hence, a second "detection laser" with less intensity, but shorter wavelength, to yield a larger amount of backscattered light for detection is commonly used.[12,14,16] This is realized by merging both laser pathways with dichroic mirrors—a critical and delicate issue since both lasers have to be spatially focused onto the same spatial position with highest precision. Then, the backscattered light has to be separated for detection from the incident and the trapping laser beam.

First attempts have been reported to detect backscattered light of the trapping laser, first, by means of a nonpolarizing beam splitter that deflects a fraction of the backscattered light from the trapped object,[11,13] and second, by an approach, where the backscattered light was extracted by a combination of a polarizing beam splitter and a quarterwave plate (QWP).[17]

Since we aim for quantitative single molecule experiments at membrane surfaces containing nanopores,[18] a versatile optical tweezer system to integrate an appropriate liquid cell is mandatory. Because all of the mentioned techniques strongly suffer from interference effects resulting from the superposition of backscattered light from the bead and from a weakly reflecting surface (e.g., water-glass surface of the liquid cell),[14,19] we developed a single beam optical tweezers setup in reflection mode based on an inverted optical microscope where an appropriate spatial filtering was introduced. In our setup, the backscattered light serves for position detection in three dimensions with remarkably high precision, which is proved by overstretching single DNA molecules in the *x* direction (perpendicular to the optical axis)[20,21] and in the *z* direction (along the optical axis).[22] The spatial filtering that relates to a recently described technique,[23,24] particularly yields a very stable force signal in the *z* direction, which is only weakly affected by unwanted interference effects when operated in the vicinity of a low reflective solid state membrane containing a nanopore.[14,25,26] Exemplarily, the translocation of a single DNA molecule through this nanopore[14,27] can precisely be monitored as the molecule is immobilized on a microbead only a few micrometer beneath the membrane, or when the distance between bead and membrane is varied.

[a)]Author to whom correspondence should be addressed. Electronic mail: andy.sischka@physik.uni-bielefeld.de.

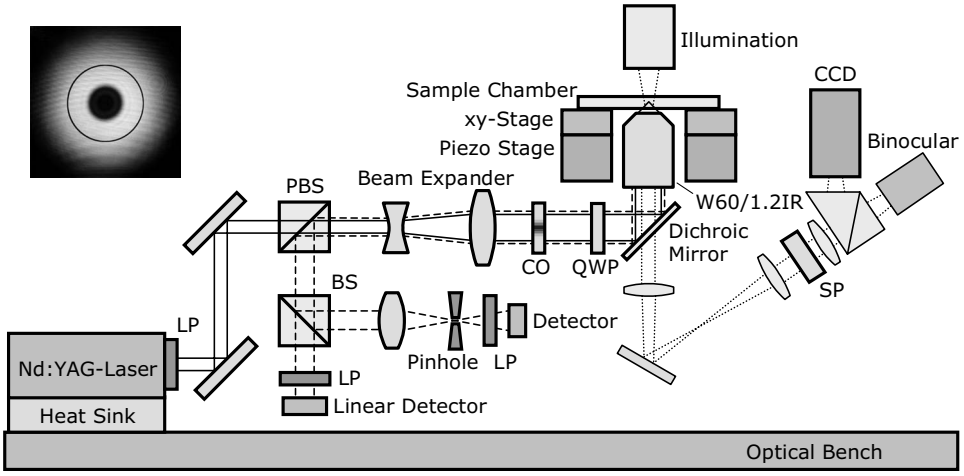

FIG. 1. Single beam optical tweezers setup. The backscatter mode of operation allows easy access to a fluid cell on top of the stage in a stable, precise, and versatile manner. The backscattered light for detection is indicated by the dashed line. Abbreviations: LP: 1064 nm long pass filter. BS: 50/50 beam splitter cube. PBS: Polarizing beam splitter cube. SP: Short pass filter for visual light. QWP: Quarterwave plate. CO: Central obstruction filter. Inset: Image of the obstructed laser beam profile before it enters the trapping objective (the thin black ring indicates the objective's back aperture of 5.7 mm diameter).

II. OPTICAL TWEEZERS SETUP

The optical tweezers system is adapted from our previously described forward scatter mode setup,[8,21] and was redesigned to allow versatile force measurements with backscattered light detection mode in three dimensions (Fig. 1).

The Nd:YAG laser (LCS-DTL-322, Laser 2000, Germany; 1064 nm, 1 W, linear polarized, TEM_{00} mode) on a passive copper heat sink is mounted on an air-damped optical bench (VH-3660W-OPT, Newport, CA). Passing a 1064 nm long pass filter (RG850, Linos, Germany) and redirected by two laser-line mirrors (10D20-ER.2, Newport, CA), the *p*-polarized beam enters the polarizing beam splitter cube (Linos, Germany) and leaves it unaffected. The beam is expanded by a factor of 6 (beam expander S6ASS106, Sill Optics, Germany) to a diameter of about 9 mm for overfilling the back aperture of the water immersion trapping objective (5.7 mm diameter) with a numerical aperture of 1.2 (UPL-APO60W/IR, Olympus, Japan). Before that, the beam passes a QWP (RM-1/4-1046, Newport, CA), changing the linearly polarized into right-circular polarized light, which is afterward reflected by a dichroic mirror (TFP1064nm56°, Laseroptik, Germany).

The homebuilt liquid cell[8] can be coarse adjusted and fully controlled with micrometer precision by a dedicated manual stage, and additionally position controlled with nanometer precision by a piezostage (P-517.3CD, Physik Instrumente, Germany) during the experiments.

For eye and camera safety, two short pass filters (KG5, Schott, Germany) are placed in the path of the visible light (dotted line in Fig. 1), right in front of the beam splitter inside the Axiovert 100 microscope (Zeiss, Germany).

The right-circular polarized beam not only generates a trapping potential that is isotropic in the *x* and *y* directions, but also enables a highly efficient force detection method: the backscattered light from the trapped particle (now left-circular polarized) is being collected by the trapping objective that changes it into a parallel light beam taking the opposite direction through the tweezer system (dashed line in Fig. 1). The QWP changes it into linear *s*-polarized light, orthogonal to the polarizing plane of the incident light.[17] After passing the beam expander, the backscattered light is reflected (>98%) by the polarizing beam splitter cube. For force measurements in the *x* and *y* directions, this light can be projected through a 1064 nm long pass filter (RG850, Linos, Germany) onto a one-dimensional (1D) or two-dimensional linear detector (in our setup: a 1D detector "1L2,5_CP1" from Laser Components, Germany), mounted on two linear stages (Newport, CA) for fine adjustment. The signal is amplified, low pass filtered (20 kHz) by a homebuilt electronic device, digitized (PCI-6036E, National Instruments, TX) and monitored under LABVIEW.

Compared to quadrant detectors, a linear detector has the advantage of a much larger linear detection range, which is required whenever the trapped bead is strongly displaced in the optical trap due to a large external force acting on the bead.[13] In our setup, the lateral displacement of the bead in the optical trap can cause a lateral displacement of the backscattered light beam on the detector that is larger than the radius of the beam itself.

Measuring the force along the optical axis (*z* direction) is basically realized by detecting the intensity of the backscattered light. Hence, an additional nonpolarizing beam splitter (50/50 beam splitter cube; Linos, Germany) is placed between the polarizing beam splitter cube and the linear detector. For standard force measurement in the *z* direction, this beam is directly projected through a 1064 nm long pass filter (RG850, Linos, Germany) onto a photodetector (SD172-11-21-221, Laser Components, Germany). A change in the light intensity can directly and linearly be related to the *z* position of the trapped bead.

For more demanding *z*-force measurements (e.g., in the vicinity of a membrane containing a nanopore), the backscattered light has to be spatially filtered, so that the amount of backscattered light coming from other surfaces is strongly reduced.[14] Therefore, a convex lens ($f=10$ mm; Linos, Germany) projects the beam in a confocal manner through a pinhole (15 μm diameter; Edmund Optics, NJ) that is mounted on three linear stages (Newport, TX) for fine adjustment.

An additional spatial filtering in the form of a central obstruction (CO in Fig. 1), similar to a circular opaque disk,[23] suppresses that light, which is backreflected from a small region around the optical axis from low reflective boundary layers (e.g., glass/water surfaces inside the liquid

cell), that otherwise give rise to unwanted interference effects.[14,19] The CO filter not only blocks the central part of the incoming laser light to form a ringlike laser beam profile[28] (see inset in Fig. 1) but also considerably blocks the disturbing backscattered light arising from surfaces on or close to the optical axis.

The obstruction filter was fabricated by evaporating gold through a 1.9 mm hole onto an antireflection coated optical window (Linos, Germany), until an opaque circular layer (1.1 mm radius) with 50 nm thickness has been deposited (distance between hole and window was 10 mm). This structure has an edge of about 0.4 mm where the opacity decreases gradually to reduce diffraction effects. Additionally, both the QWP and the CO are tilted by 1° to prevent spurious light reflections reaching the detectors or the laser.

III. FORCE CALIBRATION

Quantitative forces were calibrated in three dimensions by trapping individual microbeads suspended in the liquid cell and by moving the piezostage with a defined velocity in all directions while recording the force signal that was calibrated with the hydrodynamic friction according to Stokes' law.[29] Monodisperse streptavidin-coated beads (3.28 μm diameter; Spherotech, IL; concentration of 0.5% w/v) that were suspended by a factor of 1:2500 in phosphate buffered saline (PBS) buffer, consisting of 136 mM NaCl, 2.7 mM KCl, 8.1 mM Na_2HPO_4, and 1.5 mM KH_2PO_4 at pH 7.4, with additional 1 mM of EDTA were used. These beads are large enough not to suffer from interference effects such as axial trap stiffness variations that are generated by partially backreflected laser light on internal surfaces of the liquid cell.[30] The calibration, as well as all of the following experiments was performed at room temperature (21 °C).

IV. CHARACTERIZING THE SETUP

In backscatter mode, the trapping objective acts as condenser objective that permits the integration of a variety of dedicated setups and liquid cells above the trapping objective without influencing the measurement of small forces in the subpiconewton range.

In the following, the given laser power output (LPO) refers to the power at the laser aperture. At 1000 mW LPO, the power inside the optical trap is 295 mW with CO, and 410 mW without CO. Unlike other single-laser systems working in backscatter mode,[11,13] the amount of backscattered light in our setup is 3 mW (measured at the 50/50 beam splitter cube) with no CO installed, and 1.4 mW with installed CO (at 1000 mW LPO), which is more than sufficient to distribute it onto both detectors. The maximum trapping force without CO is 360 pN in the x direction and about 90 pN in the z direction. With the CO, we can achieve a maximum trapping force of 220 pN in the x direction and about 75 pN in the z direction at 1000 mW LPO.

For testing and comparing the functionality of force measurements in the x direction, experiments were performed with both the forward[8,21] and backscatter mode setups for simultaneous measurements without using the CO. As seen in Fig. 2(a), there was no significant difference when

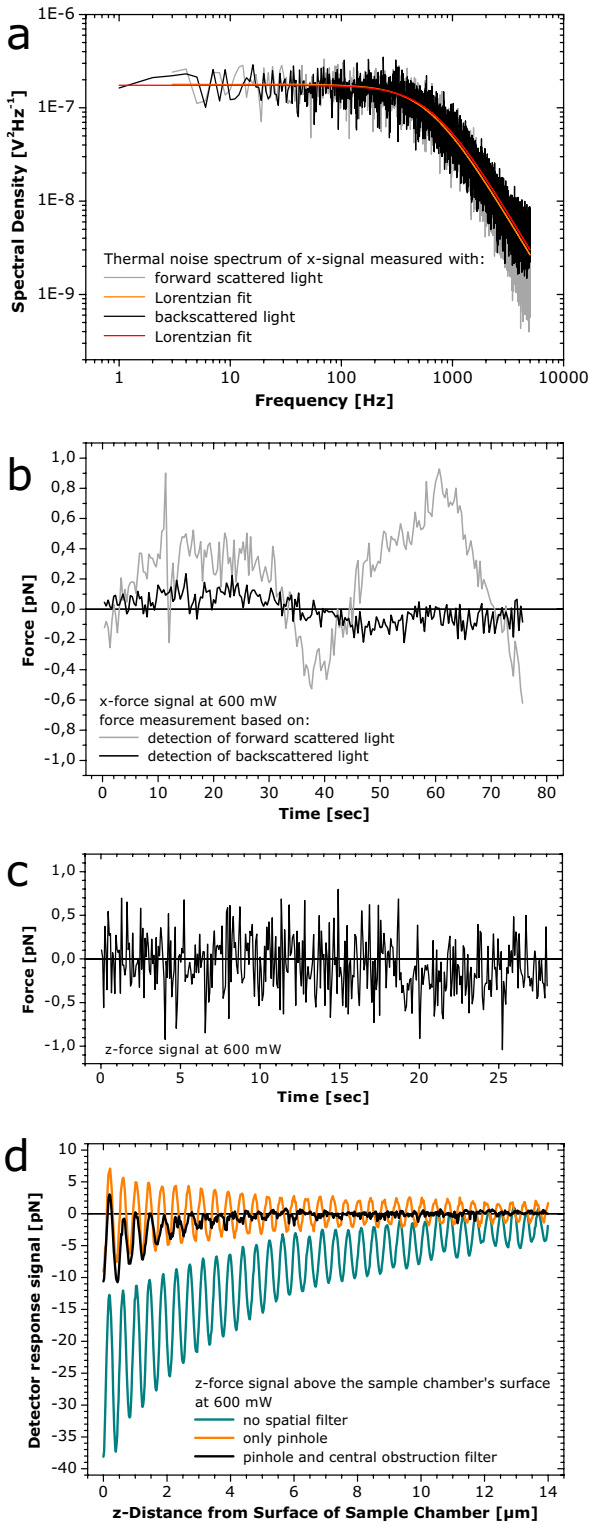

FIG. 2. (Color online) Signal performance. (a) Thermal noise spectrum of the x-detector signal of a trapped bead (diameter: 3.28 μm), measured with forward scattered light and backscattered light detection at 600 mW laser power output. (b) The long time stability and low frequency noise level of the lateral force signal (bandwidth of 40 Hz) was found to be more favorable in the backscatter mode of operation. (c) The z-force signal measured in backscatter mode, with the pinhole and the CO being installed, yielded an overall peak-to-peak noise signal of 1 pN (bandwidth of 40 Hz). (d) The z-detector response signal, depending on the z distance between the lower surface of the bead and the bottom of the liquid cell. The effect of spatial filtering with the CO considerably reduces the disturbing interference effect between the backscattered light from the bead and from the weakly reflecting surface of the liquid cell.

characterizing the optical trap using the thermal noise spectrum of a trapped bead in the absence of an external force. However, advantageous for the backscatter mode is that vertical movements of the trapping objective due to required focusing or mechanical drift has no functional influence on the calibration and resolution of the tweezers system, as it can be seen in the long term stability of the base line signal of a trapped bead [Fig. 2(b)]. The backscattered light path is more insusceptible against thermal or mechanical drift and misalignments, yields increased long term stability, and better tolerates the beam pointing instability that each laser has.[31] This instability becomes noticeable as a periodical artifact within the force signal as a result of the laser beam that rotates around an elliptical based cone, causing a lateral displacement and an orbiting of the laser focus of several nanometers around the trapping objective's optical axis. The backscatter setup has advantages that can lead to a great insusceptibility against the beam pointing instability, which is discussed in details elsewhere.

Figure 2(c) shows the z-force signal of a trapped bead without an external force as the CO and the pinhole has been installed. Backscattered light from other surfaces than the trapped bead can be ignored, as long as it has a constant intensity, e.g., when moving the bead only in the x or y directions. However, the obstruction filter becomes essential when moving the bead in the z direction, perpendicular to a weak reflecting surface inside the liquid cell. The backscattered light from the bead and from the surface generates an interference effect that causes an oscillation of the z-detector response signal.[14] The position of the trapped bead is basically not affected by this interference effect, since the low amount of backscattered light from another surface than the trapped bead has no significant influence onto the absolute position of the trapped bead. Instead of that, this interference effect basically affects the detector response signal, which can be clearly emphasized when displaying this signal artifact in terms of force. This effect was examined, as the bead was approached to the bottom of the liquid cell with a velocity of 0.3 μm/s. Because no noticeable net force in the z direction was generated, one would expect no change within the z detector signal until the bead will touch the surface. However, when approaching the bottom, the weak reflectivity of the liquid cell's bottom surface increases the interference effect, that becomes noticeable as an oscillating detector response signal. This result is shown in Fig. 2(d), where we present the z signal (given in terms of force) without any spatial filtering, when using only the pinhole as a spatial filter, and when using both the pinhole and the CO, respectively. Mere pinhole filtering reduces the interference effect by a factor of 2, which is in agreement with previous measurements on Si_3N_4 membranes,[14] whereas additional spatial filtering with the CO again improves the reduction by a factor of up to 4.

We found that upon increasing the diameter of the CO, a further reduction in the interference can be observed that, however, is accompanied with a decreased trapping power. In order to determine the trap stiffness in the x and z directions, with and without CO, as well as the absolute axial position resolution, we let one bead adhere on the bottom of the liquid cell, and pulled the bead through the laser focus while recording both the detector signals and the position data of the piezostage. Regarding the axial resolution, the bead was positioned in the center of the trap and moved rectangularly with an amplitude of 10 nm in the z direction. The associated detector response signal is shown in Fig. 3(a), where these steps can clearly be distinguished with a resolution of 2 nm.

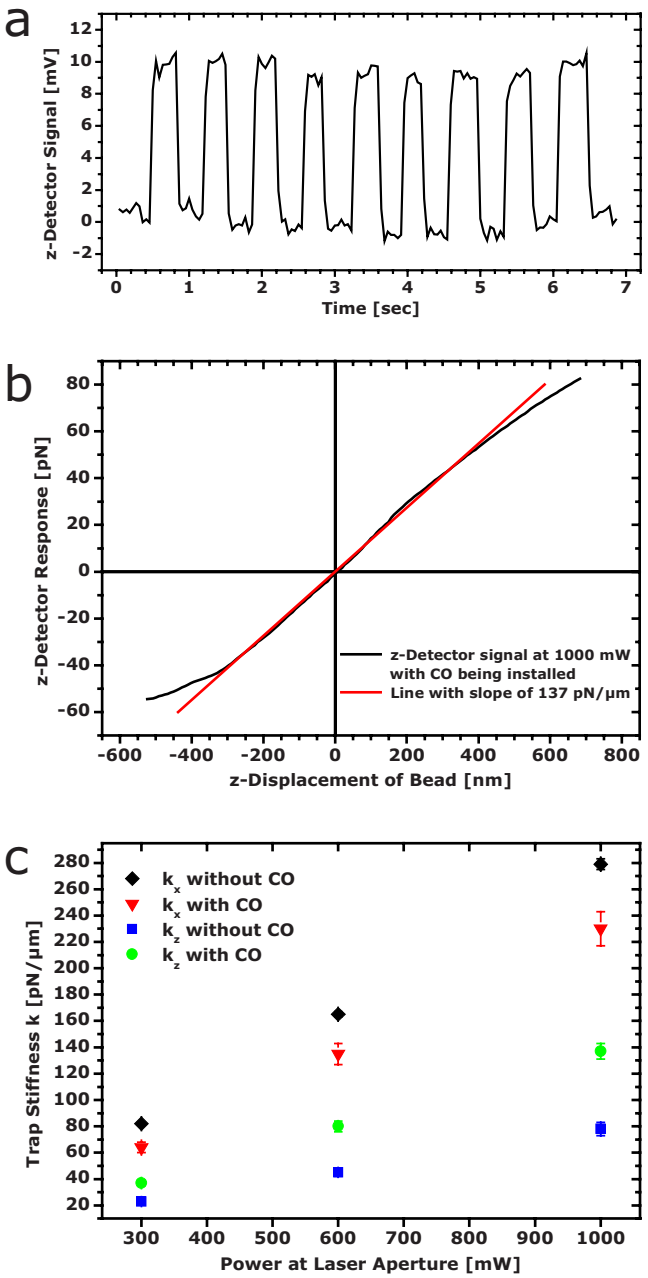

FIG. 3. (Color online) (a) Detector response signal (25 Hz bandwidth) of a bead, which was moved periodically in a rectangular waveform with an amplitude of 10 nm in the z direction through the center of the optical trap, with a resolution of 2 nm (0.95 mV equals 1 nm). The bead was immobilized on the bottom of the liquid cell and the CO was installed. (b) Pulling the immobilized bead through the optical trap in the z direction yields a linear detector response range from −40 to +60 pN (−300 to +450 nm) at 1000 mW as the CO was installed [trap stiffness: 137 pN/μm (red line)]. (c) Trap stiffness in the x and z directions for different laser power outputs, with and without installed CO (for details, see text).

The trap stiffness in the x and z directions (with and

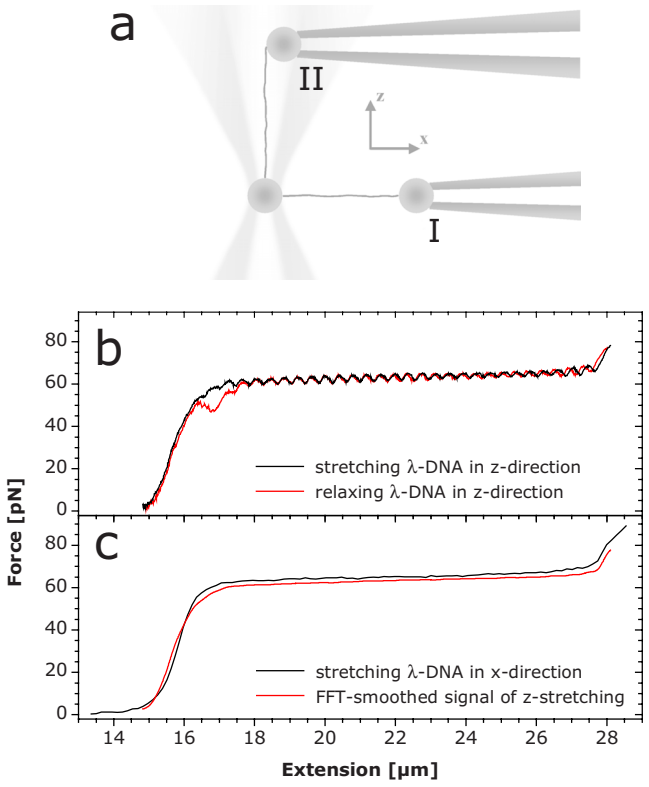

FIG. 4. (Color online) Stretching DNA. (a) Configuration for overstretching DNA in the x direction (I) and along the optical axis in z direction (II). (b) Subsequent stretching and relaxation of DNA in the z direction. The characteristic overstretching transition (plateau at $F \sim 62$ pN) can clearly be identified although weak signal oscillations within the z-detector signal are superimposed. (c) These oscillations can be (e.g., frequency domain—FFT) filtered yielding an almost identical result like the interference unaffected stretching result measured in the x direction.

without the CO) can be calculated by moving the bead in the x or z directions entirely through the optical trap, while recording the piezostage and the detector response signals. Especially in the z direction, with installed CO, we found out that the range in which the detector responds linearly to the displacement of the bead is somewhat larger for the $+z$ direction than for the $-z$ direction (from -300 to $+450$ nm at 1000 mW) [Fig. 3(b)]. Without CO, the linear range lies between -250 and $+250$ nm. In the x direction and without CO, we found a linear range from -350 to $+350$ nm. However, with installed CO, the linear range decreases (-150 to $+150$ nm), which can be attributed to a nonharmonic trap potential for larger bead displacements. In practical, the latter case can be neglected, since there is no need to install the CO when measuring forces in the x direction.

Conclusively, we calculated the trap stiffness for the x and z directions for different laser powers, with and without CO [Fig. 3(c)]. It is worth noting and advantageous to find an apparently higher trap stiffness in the z direction with installed CO, than without CO, although the maximum trapping force is larger without CO.

V. OVERSTRETCHING λ-DNA

The λ-DNA-preparation protocol, buffer, microbeads, and the approved immobilization procedure for tethering the λ-DNA between two beads for force measurements in the x direction [Fig. 4(a) (I)] were described previously.[8] For stretching λ-DNA in the z direction,[22] the DNA is immobilized between two beads in the same way as for the x-direction measurements to have the DNA elongated along the optical axis [Fig. 4(a) (II)]. With installed CO, overriding the laser power supply yields a laser power output of 1.2 W that is necessary for achieving a maximum z force of 85 pN to pull the DNA beyond its overstretching plateau.

Overstretching DNA exhibits the well described overstretching force plateau at 64 and 62 pN for the x and z measurements, respectively [Figs. 4(b) and 4(c)],[6,20] which is in very good agreement with previous measurements in the x direction under similar conditions (temperature, ionic strength, and pH value).[6,21,32,33] Subsequent relaxation causes the relaxation hysteresis effect.[6,20]

Although the z-force detector signal is spatially filtered with the CO, it is still affected by a small oscillation artifact of the detector response signal due to the interference effect. This artifact can be treated using an appropriate fast Fourier transform (FFT) algorithm (e.g., "FFT smoothing" under Origin™, Microcal Software Inc., MA) with a cutoff frequency according to $f_c = 1/n\Delta t$, where n is the number of data points and Δt is generally the spacing between two adjacent data points. Here is, in terms of length, $n\Delta t = 0.28$ μm.

In this experiment, the main component of disturbing backreflections emerged from the second bead and the glass micropipette. Additionally, as the trapped bead is strongly deflected in the $+z$ direction, the forward scattered light beam narrows[28] and the illuminance of the second bead and the micropipette is increased.

Overlaying the two results of λ-DNA overstretching (in the x direction, and FFT-smoothed z direction) exhibit the precision of the z measurements that can be achieved with designated spatial filtering, and open the possibility of further experiments.

VI. LIQUID CELL FOR NANOPORES

We used commercial silicon supports (disks of 3 mm diameter, thickness of 200 μm; #4163SN-BA, Structure Probe Inc., PA) that contain a membrane window (20 nm thin Si_3N_4 membrane window with a size of 20×30 μm^2—indicated as 50×50 μm^2 by the manufacturer) as a carrier for nanopores. One nanopore with a diameter of 80 nm [right inset in Fig. 5(b)] was milled into the membrane using a focused ion beam (XB 1540 EsB, Zeiss, Germany).

The liquid cell [(Fig. 5(a))] consists of an aluminum rack and a glass slide ($60 \times 24 \times 0.14$ mm^3) with a 40 μm thin layer of spin coated polydimethylsiloxane (PDMS). A channel, 0.5 mm wide and 26 mm long was cut out of this layer, connecting reservoir 1 with reservoir 2. Glass slide and a second PDMS layer ($10 \times 35 \times 0.04$ mm^3) were treated 30 s in oxygen plasma to make both surfaces hydrophilic.[34] A hole with 1 mm diameter was cut into the center of the second layer, and this membrane was placed carefully onto the channel. At both ends, two 3 mm reservoir holes were punched, and the channel was filled with distilled water.

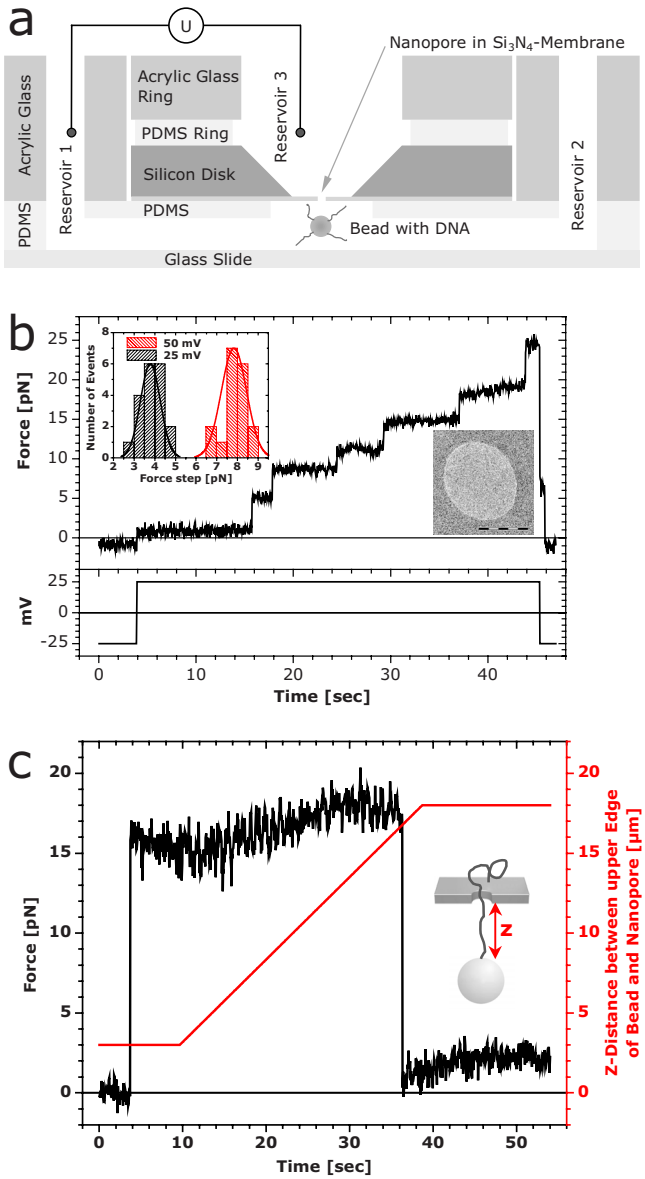

FIG. 5. (Color online) (a) Setup of the liquid cell as used for the nanopore experiments. (b) Threading of several DNA molecules into the nanopore. Each DNA molecule that was pulled into the nanopore generates an individual force step. Upon reversing the voltage again, all DNA molecules are almost instantaneously pushed out of the nanopore. Left inset: force histogram of all force steps for voltages of +25 and +50 mV. Maxima at 3.8 and 7.8 pN, respectively, prove the linear dependency between voltage and force. Right inset: transmission electron microscopy image of a 80 nm nanopore (scale bar: 50 nm). (c) Active pulling of a single λ-DNA molecule out of the nanopore (voltage: +100 mV) upon linearly increasing the bead-membrane distance from 3.0 to 18.0 μm (red line). The force signal (recorded with 100 Hz bandwidth) was almost instant and showed only weak force oscillations of about 2.5 pN due to the interference between the light backscattered from the bead and from the membrane. The DNA was completely pulled out of the nanopore at a distance of 16.8 μm.

To prevent air bubbles being formed at the membrane, the silicon disk was first immersed into isopropanol, and subsequently rinsed with distilled and properly degassed water. Then, it was pulled out of the water with a droplet remaining on the upper side of the disk, covering the pit, and after that, the disk was placed carefully onto the 1 mm hole at the center of the channel. A polymethyl methacrylate (PMMA) block with two 3 mm holes as reservoirs was used to cover and fix the channel to the rack. A PDMS ring seals the silicon disk, and a PMMA ring forms reservoir 3. Embedded magnets hold the rack tightly on the *xy* stage.

We used silver wires as electrodes that were coated with a thin layer of silver chloride by electroplating. For applying voltage to the reservoirs, a patch-clamp amplifier (Axopatch 200B, Molecular Devices, CA) operated in voltage-clamp mode was used. The entire liquid cell, as well as the headstage of the Axopatch amplifier was shielded by a Faraday cage.

VII. PREPARATION OF DNA-BEAD CONSTRUCTS

λ-DNA (48502 base pairs, 16.4 μm contour length; Promega Corp., WI) labeled with a single biotin on one end and a single digoxigenin on the other end is prepared as follows: 66 μl of λ-DNA (New England Biolabs Inc., MA) is denaturated for 15 min at 75 °C, and cooled down for 5 min on ice. 10 μl buffer with 50 mM tris/HCl, 10 mM $MgCl_2$, 10 mM DTT, 1 mM ATP, and 25 μg BSA is added, as well as 3.4 μl of 5′-GGG CGG CGA CCT-3′-biotin oligonucleotide (Thermo Hybaid Inc., NM), 3.4 μl of 5′-AGG TCG CCG CCC-3′-digoxigenin oligonucleotide (MWG Biotech AG, Germany), and 17.2 μl pure water. This solution was incubated for 1 hour at 50 °C.

Removal of strand nicks was done by adding 3.4 μl T4 ligase (New England Biolabs Inc., MA), 10 μl ATP, and subsequent incubation for 30 min at 25 °C. For purifying the biotin-DNA-digoxigenin molecules, the solution was washed by using a NICK column (Amersham Pharmacia Biosciences, UK), and stored as a DNA solution of 73 μg/μl in PBS buffer. For the preparation of constructs, where DNA is attached with its biotin end to the bead, 5 μl bead stock solution, 10 μl PBS buffer, and 0.2 μl of biotin-DNA-digoxigenin solution is incubated for 2 h at 6 °C, washed by centrifugation, and resuspended by a factor of 1:1000 in buffer (100 mM KCl, 10 mM tris/HCl, and 1 mM EDTA, *p*H 9.5).

VIII. PULLING DNA INTO THE NANOPORE

Bead-DNA constructs were first prepared with five times concentrated DNA solution, to attach several DNA molecules (typically about 5–10) at one bead. All nanopore experiments were performed in KCl buffer (100 mM KCl, 10 mM tris/HCl, and 1 mM EDTA, *p*H 9.5). A single bead was navigated beyond the horizontally orientated nanopore membrane by adjusting the fluid levels in reservoirs 1 and 2. The vertical distance between the membrane and the top surface of the bead was controlled and determined with a precision of 100 nm by monitoring the *z*-force signal until the bead slightly touched the membrane. Then, the bead was positioned 3.0 μm beneath the membrane, laterally coarse positioned with respect to the nanopore, and positive voltage (typically +25 mV) was applied to reservoir 3. The electrostatic threading of negatively charged λ-DNA molecules one by one into the nanopore is discernible by distinct force steps in the *z*-force signal [Fig. 5(b)].[14] In order to accurately determine the lateral position of the pore, the optical trap was switched off, and the bead was automatically pulled toward

the nanopore. By this procedure, lateral nanopore position detection with a precision of 200 nm was achieved. After switching on the optical trap again, the bead could always be detached vertically from the membrane in precise alignment with the nanopore.

Statistical analysis of the DNA threading events, where all force steps were plotted into a histogram [left inset in Fig. 5(b)], yields most probable force steps of 3.8 and 7.8 pN for voltages of +25 and +50 mV, respectively, and a linear dependency between force increment and applied voltage.

A last experiment was conducted, where only one DNA molecule was attached per bead. When the bead was placed 3.0 μm beneath the nanopore, a single force step of 16 pN was observed [black line in Fig. 5(c)] as a voltage of +100 mV was applied. In order to investigate the dependence of the z-force signal on the membrane as a low reflective surface, we increased the distance between bead and membrane from 3.0 to 18.0 μm [red line in Fig. 5(c)]. A rather constant z-force signal of 16 ± 2.5 pN is apparent, in which the remaining detector interference effect is only of the same order as the thermal noise fluctuations of the trapped bead (bandwidth: 100 Hz), favorably proving the technical concept of the tweezer setup. When reaching a z distance of 16.8 μm, the DNA was completely pulled out of the nanopore, a distance that complies well with the molecular contour length of λ-DNA.

IX. CONCLUSION AND OUTLOOK

A versatile and stable single beam optical tweezers system that is capable for force measurements in three dimensions that is completely based on detection of backscattered light is presented. An appropriate spatial filtering in the form of a central obstruction filter allows to strongly suppress the disturbing interference effects when operating micron-sized beads in the vicinity of weak reflective surfaces. A z-force resolution of 1 pN at a bandwidth of 40 Hz, when threading DNA molecules into a nanopore, and a resolution of about 2.5 pN, while changing the distance between bead and membrane, could be achieved.

Since the reflectivity of the Si_3N_4 membrane is the crucial part of the experiment, a further improvement of the z-force resolution by using thinner membranes is possible. The used membrane (thickness: 20 nm) has a reflectivity of 1.08% (for p-polarized light under 0° incident angle; membrane surrounded by water) as calculated by using Fresnel formalism.[35] A further reduction in the disturbing interferences will be achieved by decreasing the thickness of the membrane to 15 or 10 nm (0.62% and 0.28% reflectivity, respectively).

ACKNOWLEDGMENTS

We gratefully acknowledge helpful discussions and technical advice for the preparation and handling of the nanopores from Ulrich F. Keyser, Urs Staufer, Harald Fuchs, and Cees Dekker. We thank Sebastian Horstmeier for his calculations of Si_3N_4 membrane reflectivity and Martin Hegner for support in the early stage of this work. This work was financially supported by the Collaborative Research Center SFB 613 from the Deutsche Forschungsgemeinschaft (DFG).

[1] A. Ashkin, J. M. Dziedzic, J. E. Bjorkholm, and S. Chu, Opt. Lett. **11**, 288 (1986).
[2] S. B. Smith, Y. Cui, and C. Bustamante, Science **271**, 795 (1996).
[3] F. Gittes and C. F. Schmidt, Opt. Lett. **23**, 7 (1998).
[4] S. Yamada, D. Wirtz, and S. C. Kuo, Biophys. J. **78**, 1736 (2000).
[5] G. J. Wuite, R. J. Davenport, A. Rappaport, and C. Bustamante, Biophys. J. **79**, 1155 (2000).
[6] M. C. Williams, J. R. Wenner, I. Rouzina, and V. A. Bloomfield, Biophys. J. **80**, 874 (2001).
[7] S. Husale, W. Grange, and M. Hegner, Single Mol. **3**, 91 (2002).
[8] A. Sischka, R. Eckel, K. Tönsing, R. Ros, and D. Anselmetti, Rev. Sci. Instrum. **74**, 4827 (2003).
[9] J. P. Rickgauer, D. N. Fuller, and D. E. Smith, Biophys. J. **91**, 4253 (2006).
[10] M. J. Lang, C. L. Asbury, J. W. Shaevitz, and S. M. Block, Biophys. J. **83**, 491 (2002).
[11] M. E. J. Friese, H. Rubinsztein-Dunlop, N. R. Heckenberg, and E. W. Dearden, Appl. Opt. **35**, 7112 (1996).
[12] G. V. Soni, F. M. Hameed, T. Roopa, and G. V. Shivashankar, Curr. Sci. **83**, 1464 (2002).
[13] J. H. G. Huisstede, K. O. van der Werf, M. L. Bennink, and V. Subramaniam, Opt. Express **13**, 1113 (2005).
[14] U. F. Keyser, J. van der Does, C. Dekker, and N. H. Dekker, Rev. Sci. Instrum. **77**, 105105 (2006).
[15] K. Svoboda and S. M. Block, Annu. Rev. Biophys. Biomol. Struct. **23**, 247 (1994).
[16] G. V. Shivashankar, G. Stolovitzky, and A. Libchaber, Appl. Phys. Lett. **73**, 291 (1998).
[17] A. R. Carter, G. M. King, and T. T. Perkins, Opt. Express **15**, 13434 (2007).
[18] R. M. M. Smeets, U. F. Keyser, D. Krapf, M. Y. Wu, N. H. Dekker, and C. Dekker, Nano Lett. **6**, 89 (2006).
[19] A. Jonas, P. Zemanek, and E. L. Florin, Opt. Lett. **26**, 1466 (2001).
[20] J. R. Wenner, M. C. Williams, I. Rouzina, and V. A. Bloomfield, Biophys. J. **82**, 3160 (2002).
[21] A. Sischka, K. Tönsing, R. Eckel, S. D. Wilking, N. Sewald, R. Ros, and D. Anselmetti, Biophys. J. **88**, 404 (2005).
[22] C. Deufel and M. D. Wang, Biophys. J. **90**, 657 (2006).
[23] M. Gu, D. Morrish, and P. C. Ke, Appl. Phys. Lett. **77**, 34 (2000).
[24] K. Dholakia, P. Reece, and M. Gu, Chem. Soc. Rev. **37**, 42 (2007).
[25] A. J. Storm, J. H. Chen, X. S. Ling, H. W. Zandbergen, and C. Dekker, Nat. Mater. **2**, 537 (2003).
[26] U. F. Keyser, B. N. Koeleman, S. van Dorp, D. Krapf, R. M. M. Smeets, S. G. Lemay, N. H. Dekker, and C. Dekker, Nat. Phys. **2**, 473 (2006).
[27] E. H. Trepagnier, A. Radenovic, D. Sivak, P. Geissler, and J. Liphardt, Nano Lett. **7**, 2824 (2007).
[28] A. Ashkin, Biophys. J. **61**, 569 (1992).
[29] L. P. Ghislain, N. A. Switz, and W. W. Webb, Rev. Sci. Instrum. **65**, 2762 (1994).
[30] P. Jakl, M. Sery, J. Jezek, M. Liska, and P. Zemanek, J. Opt. A, Pure Appl. Opt. **9**, 251 (2007).
[31] A. Sischka and D. Anselmetti, "Laser beam pointing instability corrective for optical tweezers systems," (unpublished).
[32] P. Cluzel, A. Lebrun, C. Heller, R. Lavery, J. L. Viovy, D. Chatenay, and F. Caron, Science **271**, 792 (1996).
[33] M. C. Williams, I. Rouzina, and V. A. Bloomfield, Acc. Chem. Res. **35**, 159 (2002).
[34] A. Ros, W. Hellmich, J. Regtmeier, T. T. Duong, and D. Anselmetti, Electrophoresis **27**, 2651 (2006).
[35] W. N. Hansen, J. Opt. Soc. Am. **58**, 380 (1968).